CHEMISTRY
A EUROPEAN JOURNAL

DOI: 10.1002/chem.200801699

VIP

Difluorocarbene Studied with Threshold Photoelectron Spectroscopy (TPES): Measurement of the First Adiabatic Ionization Energy (AIE) of CF_2

Fabrizio Innocenti,[a] Marie Eypper,[a] Edmond P. F. Lee,[a] Stefano Stranges,[b] Daniel K. W. Mok,[d] Foo-tim Chau,[d] George C. King,[c] and John M. Dyke*[a]

Abstract: The first photoelectron band of difluorocarbene CF_2, has been studied by threshold photoelectron (TPE) spectroscopy. CF_2 was prepared by microwave discharge of a flowing mixture of hexafluoropropene, C_3F_6, and argon. A vibrationally resolved band was observed in which at least twenty-two components were observed. In the first PE band of CF_2, the adiabatic ionization energy differs significantly from the vertical ionization energy because, for the ionization CF_2^+ ($\tilde{X}^2A_1$)+e^- ← CF_2 ($\tilde{X}^1A_1$), there is an increase in the FCF bond angle (by ≈20°) and a decrease in the C–F bond length (by ≈0.7 Å). The adiabatic component was not observed in the experimental TPE spectrum. However, on comparing this spectrum with an ab initio/Franck–Condon simulation of this band, using results from high-level ab initio calculations, the structure associated with the vibrational components could be assigned. This led to alignment of the experimental TPE spectrum and the computed Franck–Condon envelope, and a determination of the first adiabatic ionization energy of CF_2 as (11.362 ± 0.005) eV. From the assignment of the vibrational structure, values were obtained for the harmonic and fundamental frequencies of the symmetric stretching mode (ν_1') and symmetric bending mode (ν_2') in CF_2^+ ($\tilde{X}^2A_1$).

Keywords: carbenes · photoelectron spectroscopy · reactive intermediates · vibrational spectroscopy

Introduction

Difluorocarbene, CF_2, is important in plasma processing and is produced in the stratosphere by photodissociation of chlorofluorocarbons by radiation from the sun. It has been studied in some detail spectroscopically in the ultraviolet,[1–4] microwave[5,6] and infrared regions.[7–10] Structural parameters of the ground state, X^1A_1, and a number of excited states have been derived from electronic emission[4] and absorption spectroscopy,[2,3] and single vibronic level (SVL) fluorescence.[1] Several microwave studies have been reported which provide precise rotational constants for the X^1A_1 state.[5,6]

Small reactive intermediates, such as CF_2, play important roles in determining the etching rate, selectivity and anisotropy of plasma-etching processes. The mechanisms of CF_2 production and destruction in fluorocarbon reactive ion-etching processes have been investigated using techniques such as laser induced fluorescence,[11] broad-band UV absorption spectroscopy,[12,13] infrared diode laser spectroscopy[14,15] and cavity-ring down spectroscopy.[16] It has been found that the primary mechanism for CF_x production (where $x = 1$, 2 and 3) is neutralisation and fragmentation of CF_x^+ ($x = 1$–4) ions incident on the powered electrode and not direct electron-impact induced fragmentation of the feedstock gas.[17] In order to understand, model and ultimately control plasmas, spectroscopic methods such as those listed above are needed to monitor reactive intermediates in plasmas, and rate-constant measurements and reaction enthalpy determinations are required for relevant reactions involving CF_2 and CF_2^+.

[a] Dr. F. Innocenti, M. Eypper, Dr. E. P. F. Lee, Prof. Dr. J. M. Dyke
School of Chemistry, University of Southampton
Highfield, Southampton SO171BJ (UK)
E-mail: jmdyke@soton.ac.uk

[b] Dr. S. Stranges
Department of Chemistry and INSTM Unit
"La Sapienza", University of Rome (Italy)
ISNM-CNR sez. Roma La Sapienza and Laboratoria
TASC-INFM-CNR
34012 Trieste (Italy)

[c] Prof. G. C. King
School of Physics and Astronomy, Manchester University
Manchester M139PL (UK)

[d] Dr. D. K. W. Mok, Prof. F.-t. Chau
Department of Applied Biology and Chemical Technology
The Hong Kong Polytechnic University
Hung Hom (Hong Kong)

The first adiabatic ionization energy (AIE) of CF_2 is important in contributing to the determination of the enthalpy of ion–molecule reactions involving CF_2^+ in plasmas. Previous determinations of the first AIE of CF_2 have included a study by vacuum ultraviolet photoelectron spectroscopy (PES),[18] which gave the first AIE as (11.42 ± 0.01) eV, a study with photoionization mass spectrometry (PIMS),[19] using radiation derived from a synchrotron source, which gave the first AIE as (11.445 ± 0.025) eV, and a study by electron impact mass spectrometry, which gave a value of (11.5 ± 0.4) eV.[20] The PES study[18] shows the first band of CF_2 to consist of regular structure, with at least fifteen components. It was interpreted[18] as a regular series in the deformation mode in the ionic state. The vertical ionization energy (VIE) was measured as (12.240 ± 0.005) eV. In the present work, this band has been re-investigated at higher resolution using threshold photoelectron spectroscopy (TPES). For this a spectrometer which has been specifically designed to study reactive intermediates with the PE and angle-resolved constant-ionic-state (CIS) methods was modified to allow TPES measurements to be performed.[21] The objective is to obtain a higher resolution spectrum of the first band of CF_2. The spectrum obtained, supported by appropriate ab initio/Franck–Condon factor calculations, should allow the first AIE to be determined more reliably than previously and enable the vibrational structure in the first band to be analysed more thoroughly.

Experimental Section

The experiments reported here were undertaken on the Circularly Polarized Beamline (4.2R, Polar) at the Elettra synchrotron radiation source (Trieste). A photoelectron spectrometer has been used which was specifically designed to study reactive intermediates with PE and CIS spectroscopy.[22–24] This spectrometer has recently been modified to allow TPE spectra to be obtained.[21] In order to record TPE spectra, the photoelectron spectrometer was tuned to detect near-zero energy (threshold) photoelectrons. The detection of threshold electrons was optimised using the $Ar^+(^2P_{3/2},^2P_{1/2})\leftarrow Ar(^1S_0)$ $(3p^{-1})$ TPE spectrum.[21,37,38] The spectral resolution obtained was typically about 5 meV as estimated from the full-width at half maximum of the main $(3p)^{-1}$ $Ar^+(^2P_{3/2})\leftarrow Ar(^1S_0)$ line. Conventional photoelectron (PE) spectra were also recorded as described in earlier work[25] and the same procedures were used to normalize the spectra for photon flux and the transmission function of the spectrometer.

CF_2 was produced by a microwave discharge of flowing hexafluoropropene, C_3F_6, diluted with argon. Preliminary experiments were carried out in Southampton in order to determine the optimum pressures which maximise the intensity of the first CF_2 band in the PE spectra. The optimum partial pressures were: $\Delta p(C_3F_6)=5\times10^{-6}$ and $\Delta p(Ar)=1\times10^{-7}$ mbar. These partial pressures were measured using an ionization gauge connected to the main vacuum chamber and are with respect to the background pressure in the vacuum chamber $(3\times10^{-7}$ mbar).

Computational Details

In order to compute potential energy functions for the ground neutral and ionic states so that Franck–Condon factors could be calculated for the first PE band of CF_2, ab initio calculations were performed. These can be described as follows:

Ab initio calculations: For the $\tilde{X}^2A_1$ state of CF_2^+, geometry optimization and vibrational frequency calculations were carried out using the restricted spin CCSD(T) method (RCCSD(T)) with augmented correlation-consistent polarized valence (aug-cc-pVXZ or AVXZ) and core-valence (aug-cc-pCVXZ or ACVXZ) basis sets of up to the quintuple-zeta (X = Q or 5) quality. With the core-valence basis sets, all electrons were correlated. For the $\tilde{X}^1A_1$ state of CF_2, ab initio total energies at different bond lengths and angles, the RCCSD(T)/aug-cc-pV5Z potential energy function (PEF) and anharmonic vibrational wavefunctions have been taken from our previous study on CF_2,[26] except for RCCSD(T)/aug-cc-pCV5Z results, which have been obtained in the present study. The largest aug-cc-pCV5Z calculations have 543 contracted basis functions.

For the evaluation of the best theoretical geometrical parameters (r_e and θ_e) and adiabatic ionization energy (AIE), the $1/X^3$ formula[27] was used to extrapolate the computed RCCSD(T)/ACVQZ and RCCSD(T)/ACV5Z values to the complete basis set (CBS) limit. Since the RCCSD(T)/ACVXZ (X = Q or 5) values were used in the extrapolation, core correlation contributions have already be accounted for. For the correction for zero-point vibrational energies (ΔZPE) in order to give AIE_0, available experimental fundamental vibrational frequencies for the $\tilde{X}^1A_1$ state of CF_2 were used.[28] For the $\tilde{X}^2A_1$ state of CF_2^+, the best theoretical ZPE was used, and it was estimated using the CBS value {extrapolation employing the $1/X^3$ formula, with the ZPEs evaluated using the computed RCCSD(T)/AVQZ and RCCSD(T)/AV5Z harmonic vibrational frequencies} plus core correlation correction {the difference between the RCCSD(T)/ACVQZ and RCCSD(T)/AVQZ values}.

Potential energy functions, anharmonic vibrational wavefunctions and Franck–Condon factor calculations: The PEF of the $\tilde{X}^2A_1$ state of CF_2^+ was fitted to 106 computed CASSCF/MRCI+D/AV5Z energies in the ranges of $0.9\le r(CF)\le1.95$ Å and $70.0\le\theta(FCF)\le160.0°$. The multi-reference CASSCF/MRCI method (including the Davidson correction, with a full valence active space) has been used in energy scans for the fitting of the PEF of the $\tilde{X}^2A_1$ state of CF_2^+ because multi-reference character becomes non-negligible in the region with $r\ge1.6$ Å. Nevertheless, computed CI coefficients of the major electronic configuration obtained from the MRCI calculation of the $\tilde{X}^2A_1$ state of CF_2^+ in this region have values larger than 0.778, and the sums of the squares of the computed CI coefficients of all reference configurations, $\Sigma(C_{ref})^2$, have values larger than 0.959, indicating that the computed MRCI wavefunctions describe the electronic state studied adequately. The root-mean-square (r.m.s) deviations of the fitted PEFs of the $\tilde{X}^2A_1$ state of CF_2^+ from computed ab initio energies is 12.9 cm^{-1}.

The details of the coordinates and polynomial employed for the PEFs, the rovibrational Hamiltonian[29] and anharmonic vibrational wavefunctions used in the variational calculations, and the Franck–Condon (FC) factor calculations which include Duschinsky rotation and anharmonicity have been described previously[26,30] and hence will not be repeated here. Nevertheless, some details of the harmonic basis functions used in the calculation of the anharmonic vibrational wavefunctions of the $\tilde{X}^2A_1$ state of CF_2^+ are given. The vibrational quantum numbers of the harmonic basis functions of the symmetric stretching and bending modes employed in the calculation of anharmonic wavefunctions have values of up to $v_1'=12$, $v_2'=25$ with the restriction of $(v_1'+v_2')\le25$.

The best computed geometry of the $\tilde{X}^2A_1$ state of CF_2^+ obtained at the CBS limit in the present study, the experimental geometry of the $\tilde{X}^1A_1$ state of CF_2 ($r_e=1.2975$ Å and $\theta_e=104.81°$, derived from experimentally derived A_e and B_e values)[31] and the experimental AIE_0 value of 11.362 eV (see later) obtained from the TPES spectrum in the present study were used in the FC factor calculations. In addition, FC factors were calculated at Boltzmann vibrational temperatures of 0 K and 600 K. The CF_2^+ $(\tilde{X}^2A_1)+e^-\leftarrow CF_2$ $(\tilde{X}^1A_1)$ photoelectron band has been simulated with these computed FC factors. The method includes allowance for Duschinsky rotation and anharmonicity. A Gaussian linewidth of 0.005 eV full-width-at-half-maximum (FWHM) was used for each vibrational component in the spectral simulation, as the experimental threshold photoelectron spectrum (TPES) has a resolution of ca. 0.005 meV FWHM.

The MOLPRO suite of programs[32] was employed for all ab initio calculations carried out in the present investigation. The PEF of the $\tilde{X}^2A_1$ state of CF_2^+ and the full list of computed FC factors of the CF_2^+ ($\tilde{X}^2A_1$) + e^- ←CF_2 ($\tilde{X}^1A_1$) photoionization process are available, upon request, from the authors.

Results and Discussion

Experimental spectra: The UV photoelectron spectrum of C_3F_6 shows a structured band in the region 10.4–11.9 eV and five broad bands in the ionization energy region 14.0–17.0 eV.[33,34] Microwave discharge of flowing C_3F_6/Ar mixtures gives rise to complete destruction of C_3F_6 with production of CF_2 and C_2F_4. It is also known from separate experiments that microwave discharge of flowing C_2F_4/Ar mixtures gives CF_2. In this work, the discharge conditions and partial pressures of C_3F_6 and Ar were optimised to give the maximum yield of CF_2. A photoelectron spectrum obtained at $h\nu = 21.0$ eV from discharged C_3F_6/Ar in the ionization region 10.0–13.2 eV showing the first bands of C_2F_4[35,36] and CF_2[18] is shown in Figure 1.

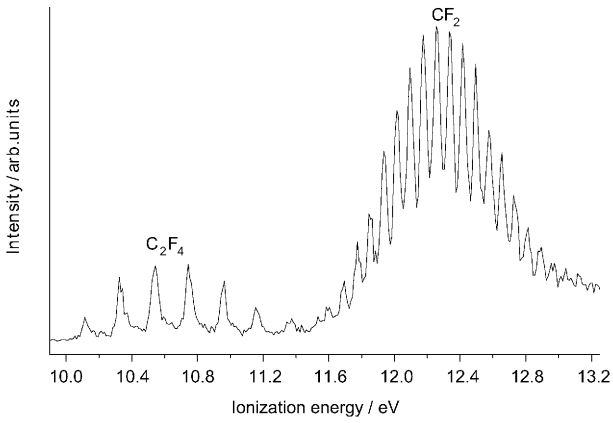

Figure 1. UV photoelectron spectrum recorded at a photon energy of 21.0 eV of a microwave discharge of a flowing mixture of hexafluoropropene, C_3F_6, in Ar. Spectra obtained under these conditions show that all the C_3F_6 is destroyed and converted into CF_2 and C_2F_4.

In order to record TPE spectra, the penetrating-field analyzer was tuned to detect near-zero energy (threshold) photoelectrons. The detection of threshold electrons was optimised using the $Ar^+(^2P_{3/2},^2P_{1/2})$←$Ar(^1S_0)$ $(3p^{-1})$ TPE spectrum.[21,37,38] The spectral resolution obtained is typically about 5 meV as estimated from the full-width at half maximum of the main $(3p)^{-1}Ar^+(^2P_{3/2})$← $Ar(^1S_0)$ band.

Figure 2 shows the TPE spectrum of CF_2 recorded in the photon region from 11.3 to 13.2 eV together with a PE spectrum recorded at $h\nu = 21.0$ eV. Whilst the observed relative intensities of vibrational components in a PE band in a conventional PE spectrum are almost always governed by Franck–Condon factors between the initial neutral and final ionic state, those observed by TPES are often dominated by autoionization.[39,40] This is primarily due to the high density of Rydberg states, which are parts of series which converge on higher rovibronic ionic levels. These can autoionize and produce electrons of low kinetic energy that are detected in TPES. As a result, autoionization processes can lead to non-Franck–Condon distributions as well as the observation of ionic vibrational levels which are not observed in the normal Franck–Condon distribution. Also, these autoionization processes may lead to observation of ionic states that cannot be observed by direct ionization from the ground state in conventional PES. The TPE spectrum in Figure 2 shows a better resolution and a very different vibrational profile with respect to the Franck–Condon distribution of the PE spectrum.

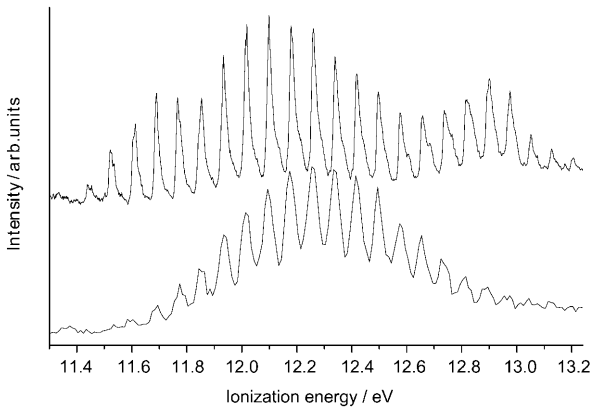

Figure 2. TPE (upper) and PE (lower) spectra recorded for a flowing CF_2 and Ar mixture in the 11.3–13.2 eV photon energy region.

In the TPE spectrum the lower vibrational bands are more intense and more clearly resolved than in the PE spectrum where the lowest vibrational component that is clearly observed is at about 11.6 eV (two additional lower-energy components were observed in the original PES study).[18] In the earlier PES study of CF_2,[18] the adiabatic and vertical ionization energies were determined as 11.42 ± 0.01 eV and 12.240 ± 0.005 eV respectively. In the present study it is possible to measure the VIE from the PE spectrum as 12.258 ± 0.002 eV and the lowest vibrational band observed in the TPE spectrum as 11.438 ± 0.004 eV. In both cases the shift with respect to the previous study[18] is 18 meV higher. From the experimental TPE spectrum, it is not possible to establish if the component observed at 11.438 eV is really the lowest vibrational component in the PE spectrum of CF_2. This is because below 11.4 eV there is a contribution from the highest observed vibrational component of the first PE band of C_2F_4 as can be seen in Figure 2 and the intensity of a lower vibrational band of CF_2, if present, would be very small compared to the noise level. Indeed in the TPE spectrum in Figure 2 it is possible to observe some structure below 11.4 eV but the signal-to-noise is not sufficient to allow unambiguous identification of weak C_2F_4 contributions and possible weak vibrational components of CF_2. For this

reason the experimental TPE spectrum was compared with an ab initio/Franck–Condon computed vibrational envelope to see if the AIE of CF_2 could be established.

Figure 3 shows the experimental TPE spectrum compared with the simulated CF_2^+ (X^2A_1)←CF_2 (X^1A_1) photoelectron spectrum at 0 K. The spectral simulation used a Gaussian function of width 5 meV for each vibrational component that is comparable with the experimental resolution. The calculated adiabatic component is placed at 11.367 eV. This was done by positioning the computed envelope so that the structure in the higher components in the TPE spectrum matches well with the computed structure, notably in the third, fourth, sixth and ninth components. The 11.36 eV

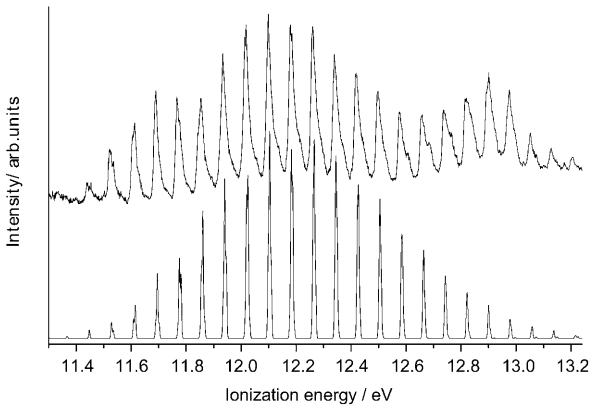

Figure 3. TPE spectrum recorded for a flowing CF_2 and Ar mixture in the 11.3–13.2 eV photon energy region (upper). Simulated CF_2^+ (X^2A_1)←CF_2(X^1A_1) photoelectron spectrum for 0 K Boltzmann vibrational temperature (lower).

component has a very small relative intensity and it is below the noise level of the experimental TPE spectrum. The positions of all the observed vibrational components are in excellent agreement with the computed components although the TPE vibrational envelope is different from the computed envelope. This is because of the non-Franck–Condon behaviour of threshold photoionization. The shape of each experimental vibrational component closely matches the shape of the corresponding calculated vibrational component as can be seen from the comparison of the lowest vibrational components shown in Figure 4. In the third, sixth and eleventh experimental vibrational components (counting the 11.36 eV component, not shown in Figure 4, as the first), it is possible to observe two features with the one at lower ionization energy more intense; the same pattern is observed in the calculated vibrational components. The fourth, seventh and ninth experimental vibrational components each show two features with the one at higher ionization energy more intense; the same pattern is observed in the calculated fourth and seventh vibrational components while in the ninth component the two contributing features are comparable in intensity. In the other calculated vibrational components in Figure 4 the 5 meV band-width used is not good enough to allow separation of different components

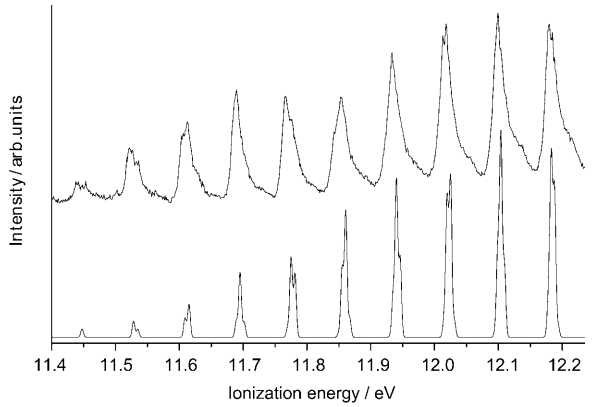

Figure 4. Expanded TPE spectrum of CF_2 in the 11.4–12.2 eV photon energy region (upper). Simulated CF_2^+(X^2A_1) ← CF_2(X^1A_1) photoelectron spectrum for 0 K Boltzmann vibrational temperature (lower).

and the same is true for the corresponding experimental vibrational components which appear to be a single feature. The exception is the vibrational component at 11.45 eV in Figure 4 which is a single vibrational component in the calculated spectrum while it appears to have two components in the experimental spectrum.

The simulated spectrum in Figure 4 was computed with a Boltzmann vibrational temperature of 0 K. The calculation has been repeated using a Boltzmann distribution at a temperature of 600 K and the result is shown in Figures 5 and 6.

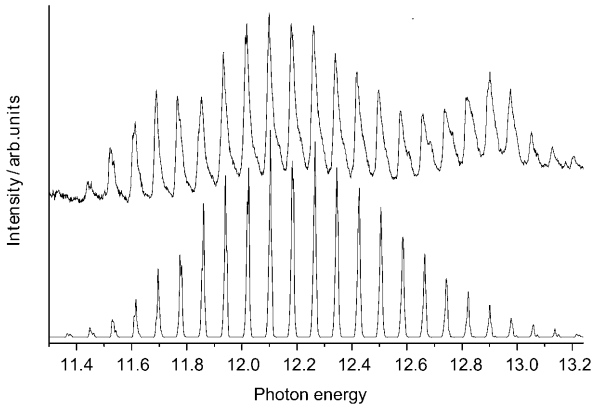

Figure 5. TPE spectrum recorded for a flowing CF_2 and Ar mixture in the 11.3–13.2 eV photon energy region (upper). Simulated CF_2^+(X^2A_1) ← CF_2(X^1A_1) photoelectron spectrum for 600 K Boltzmann vibrational temperature(lower).

The main differences with respect to the simulation at 0 K are at ionization energies above 12.8 eV and for the vibrational component in Figure 4 at ≈11.45 eV. This band, in the calculation at 600 K, has a "hot band" on the higher ionization energy side as can be seen in Figure 6. The shape of the 11.45 eV vibrational component in the experimental TPE spectrum in Figure 4 is therefore explained considering the contribution from the "hot" band. The simulated spectrum at 600 K offers an even better match with the experi-

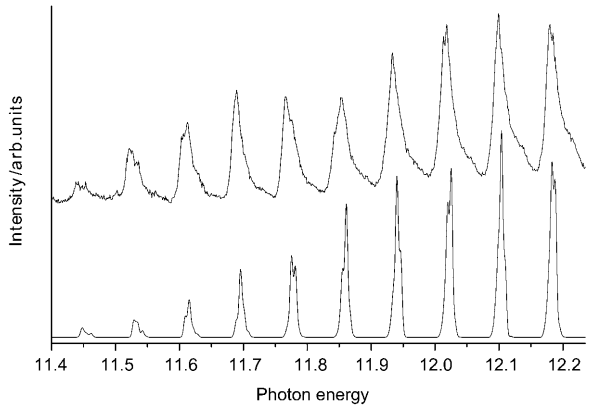

Figure 6. Expanded TPE spectrum of CF_2 in the 11.4–12.2 eV photon energy region (upper). Simulated $CF_2^+(X^2A_1) \leftarrow CF_2(X^1A_1)$ photoelectron spectrum for 600 K Boltzmann vibrational temperature (lower).

mental spectrum with respect to the simulated spectrum at 0 K. Indeed, on comparing Figure 4 with Figure 6 it is possible to notice an improvement of the agreement with the calculated spectrum at 600 K in particular for the fourth, sixth and ninth vibrational components (counting the component at 11.36 eV as the first).

The vibrational components above 12.8 eV in the TPE experimental spectrum show considerable intensity and a clear deviation from the computed Franck–Condon relative intensities. This is probably due to strongly autoionizing Rydberg states converging to higher ionic limits of CF_2. The simulation at 600 K shows some weak extra structure above 12.8 eV, due to the contributions from "hot" bands, with respect to the simulation at 0 K (compare Figure 3 with Figure 5).

The ionization energies of the calculated vibrational components from the ab initio/Franck–Condon factor calculations are on average 5 meV higher than the more intense experimental vibrational components in the 11.6–12.6 eV region. Hence, by moving the computed bands in Figure 3 by 5 meV to match the more intense experimental TPE vibrational component positions in the photon energy region 11.6–12.6 eV, we determine the AIE to be 5 meV lower than the value obtained from the simulation. This gives a value of 11.362 ± 0.005 eV for the AIE.

Ab initio results: The computed ab initio results obtained in the present study for the $\tilde{X}^2A_1$ state of CF_2^+ are summarized in Table 1, and the corresponding results obtained for CF_2 $\tilde{X}^1A_1$ are shown in Table 2. Previous MRSDCI/DZP results of Cai[41] (see references therein for earlier, lower level, ab initio results) on the $\tilde{X}^2A_1$ state of CF_2^+ are also included in Table 1. Nevertheless, since the ab initio calculations carried out in the present work are of significantly higher level and also are more systematic than previous work, we will focus only on our results in the following discussion. From Table 1, the best computed geometrical parameters of the $\tilde{X}^2A_1$ state of CF_2^+ obtained at the CBS limit (including core correlation as mentioned above) are $r_e(CF) = 1.2131 \pm 0.0006$ Å and $\theta_e(FCF) = 124.59 \pm 0.04°$. The associated uncertainties have been estimated by the differences between the CBS and RCCSD(T)/ACV5Z values. These geometrical parameters are currently the most reliable values, as no experimentally derived values are available at present.

Table 1. Optimized geometrical parameter (r_e in Å and θ_e in degrees) and computed vibrational frequencies {$\omega_1(a_1)$, $\omega_2(a_1)$ and $\omega_3(b_2)$ in cm^{-1}} of, and computed adiabatic ionization energies (IE in eV) to, the $\tilde{X}^2A_1$ state of CF_2^+, obtained at different levels of calculations.

Method	r_e	θ_e	ω	IE
RCCSD(T)/aug-cc-pVQZ	1.2168	124.63	1374.6, 648.6, 1698.9	11.3865
RCCSD(T)/aug-cc-pV5Z	1.2160	124.58	1379.1, 649.7, 1701.7	11.4010
RCCSD(T)/aug-cc-pCVQZ[a]	1.2143	124.67	1379.1, 651.2, 1704.6	11.3807
RCCSD(T)/aug-cc-pCV5Z[a]	1.2137	124.63		11.3937
CAS/MRCI/aug-cc-pV5Z	1.2185	124.63		
(as above) PEF	1.2185	124.52	1370.0, 653.2, –	
(as above) PEF, v's			1356.3, 651.7, –	
CBS (ACVQZ, ACV5Z)[b]	1.2131	124.59		11.412 ± 0.018
Δ(ZPE)[c]				+0.046
best theoretical IE_0[d]				11.458 ± 0.020
MRSDCI/DZP[e]	1.222	124.5	1259, 656, 1599	
photoion. MS[f]				11.445 ± 0.025
He I photoelectron spectrum[g]			–, 650 ± 40, –	11.42 ± 0.01
TPES				11.362 ± 0.005

[a] All electrons correlated; see text. [b] Extrapolation to the complete basis limit (CBS), employing the $1/X^3$ formula and the RCCSD(T) values calculated using the aug-cc-pCVQZ (ACVQZ) and aug-cc-pCV5Z (ACV5Z) basis sets. The estimated uncertainty for IE is the difference between the best theoretical value and the ACV5Z value. [c] Contribution of zero-point energies (ZPE) of the two states involved: For CF_2, the experimental fundamental vibrational frequencies, 1225.08, 666.25 and 1114.44 cm^{-1} (gas phase values from NIST WebBook),[28] were used, giving a ZPE value of 0.1863 eV. For CF_2^+, the CBS($1/X^3$; AVQZ, AV5Z) ZPE value of 0.2315 eV and core(AVQZ, ACVQZ) correction of +0.0008 eV give the best theoretical ZPE value of 0.2323 eV and a best estimated Δ(ZPE) value of 0.045 eV. [d] CBS+ΔZPE. [e] From ref. [41]. [f] Photoionization mass spectrometry, from ref. [19]. [g] Ref. [18].

Table 2. Computed geometrical parameters and harmonic vibrational frequencies (fundamental values in cm^{-1}) of the $\tilde{X}^1A_1$ of CF_2 obtained at the RCCSD(T) level of calculation using different basis sets. The RCCSD(T)/aug-cc-pV5Z potential energy function (PEF) and anharmonic vibrational wavefunctions used have been taken from our previous study on CF_2.[26]

RCCSD(T)	R_e [Å]	θ_e [°]	ω_1	ω_2	ω_3
Aug-cc-pVQZ	1.3008	104.786	1242 [1231]	670 [668]	
Aug-cc-pV5Z	1.2953	104.907	1247 [1234]	675 [672]	
Aug-cc-pCVQZ	1.2981	104.846			
exptl.[42]	1.2975	104.81	[1225.0793]	[666.24922]	[1114.4435]

Regarding computed harmonic vibrational frequencies of the $\tilde{X}^2A_1$ state of CF_2^+ obtained in the present study from RCCSD(T) calculations, the largest difference between

values obtained using different basis sets is less than 6 cm^{-1}. The difference between the computed symmetric stretching harmonic frequencies obtained from RCCSD(T)/AV5Z calculations and the CASSCF/MRCI/AV5Z PEF is about 9 cm^{-1}, which may be considered as the largest theoretical uncertainty associated with the computed vibrational frequencies reported in this article. Before the vibrational assignment of the TPES spectrum is considered, it should be noted that the only available experimental vibrational frequency of the $\tilde{X}^2A_1$ state of CF_2^+ is that of the bending mode, 650 ± 40 cm^{-1}, measured in the previously recorded UV photoelectron spectrum.[18] This experimental ν_2' value agrees very well with the corresponding computed value of 651.7 cm^{-1} obtained from the MRCI PEF of the present study. However, as will be shown below in the comparison between the simulated PE spectrum and the experimental TPE spectrum, the observed vibrational structure in the UV PE spectrum[18] is not due to a single ν_2' progression, but a number of combination bands. Nevertheless, the excellent agreement between the simulated PE spectrum and the observed TPE spectrum, in terms of position and shape of the individual vibrational components, indicates that the computed vibrational frequencies reported here are very close to the true values.

The best computed AIE obtained at the CBS limit in the present study is 11.412 ± 0.018 eV. Correction of zero point energies of the two states involved yields the best computed AIE_0 value of 11.46 ± 0.02 eV. This value agrees very well with the earlier experimental values of 11.445 ± 0.025 eV and 11.42 ± 0.01 eV obtained from photoionization mass spectrometry[19] and UV photoelectron spectroscopy, respectively[18] but less well with the AIE derived in this work of 11.362 eV.

Computed Franck–Condon factors and simulated photoelectron spectrum: The computed FC factors (FCFs) of the CF_2^+ ($\tilde{X}^2A_1$)+e^-←CF_2 ($\tilde{X}^1A_1$) photoionization process obtained with Boltzmann vibrational temperatures of 0 and 600 K are shown in Figure 7 (upper and lower spectra in this Figure, respectively; the computed FCF of the strongest vibrational component is set to 100 arbitrary units in all parts of this figure). The computed FCFs of vibrational "hot" bands arising from ionizations from the (0,1,0), (1,0,0), (0,2,0) and (1,1,0) levels of the $\tilde{X}^1A_1$ state of CF_2 obtained at 600 K are also shown in Figure 7 (middle spectrum). It can be seen from this Figure that "hot" band contributions to the whole simulated spectrum are small. The most noticeable contributions of "hot" bands are probably in the low IE region, relative to ionizations from the (0,0,0) level of the $\tilde{X}^1A_1$ state, as has already been discussed in the comparison between the simulated PE spectrum and the experimental TPE spectrum.

Although the vibrational structure of the previously reported UV PE spectrum[18] appears to consist of only one vibrational series, our computed FCFs show that a large number of combination bands are involved. The computed FCFs of eight major vibrational series obtained at a Boltzmann vibrational temperature of 0 K, which contribute to the CF_2^+ ($\tilde{X}^2A_1$) + e^- ← CF_2 ($\tilde{X}^1A_1$) ionization process, are shown in Figure 8. In practice, vibrational components with v_1' and/or v_2' having values of up to at least 8 for both vibrational quantum numbers have non-negligible contributions. It should be noted, however, that computed anharmonic wavefunctions of vibrational levels of the $\tilde{X}^2A_1$ state of CF_2^+ with relatively high quantum numbers show contributions from several different basis functions. Consequently, vibrational assignments of levels with v_1' and/or v_2', having values larger than 7, are tentative. Nevertheless, it is clear that the $(3,v_2',0)$←$(0,0,0)$ series is the strongest vibrational progression and the $(3,3,0)$←$(0,0,0)$ vibrational component has the largest computed FC factor (see Figure 8).

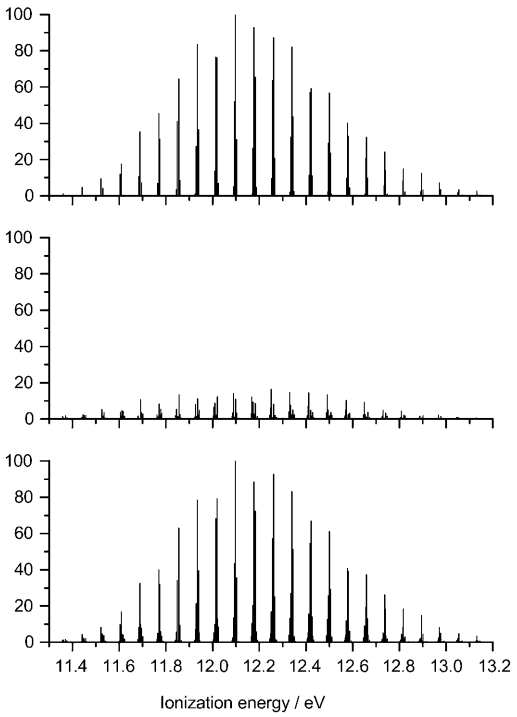

Figure 7. Computed Franck–Condon factors of the CF_2^+ ($\tilde{X}^2A_1$) + e^-←CF_2 ($\tilde{X}^1A_1$) photoionization process obtained with Boltzmann vibrational temperatures of 0 K (top trace) and 600 K (bottom trace), and those of "hot" bands arising from ionizations from the (0,1,0), (1,0,0), (0,2,0) and (1,1,0) levels of the $\tilde{X}^1A_1$ state of CF_2 (middle trace).

In Figure 9, computed FCFs in the 11.5–12.9 eV IE region at a Boltzmann vibrational temperature of 600 K and vibrational assignments of some of the relatively strong vibrational components arising from the (0,0,0) level of the $\tilde{X}^1A_1$ state of CF_2 are shown. In this IE region, some partially resolved components with a doublet structure were observed in the TPE spectrum. Computed FCFs in this region show that these doublet structures are due to $(v_1',v_2'+2,0)$←$(0,0,0)$ and $(v_1'+1,v_2',0)$←$(0,0,0)$ ionizations, because $2\nu_2'$ has a magnitude close to ν_1'.

In Figure 10, computed FC factors and assignments of some vibrational components in the adiabatic ionization region are shown. It can been seen from the Figure that

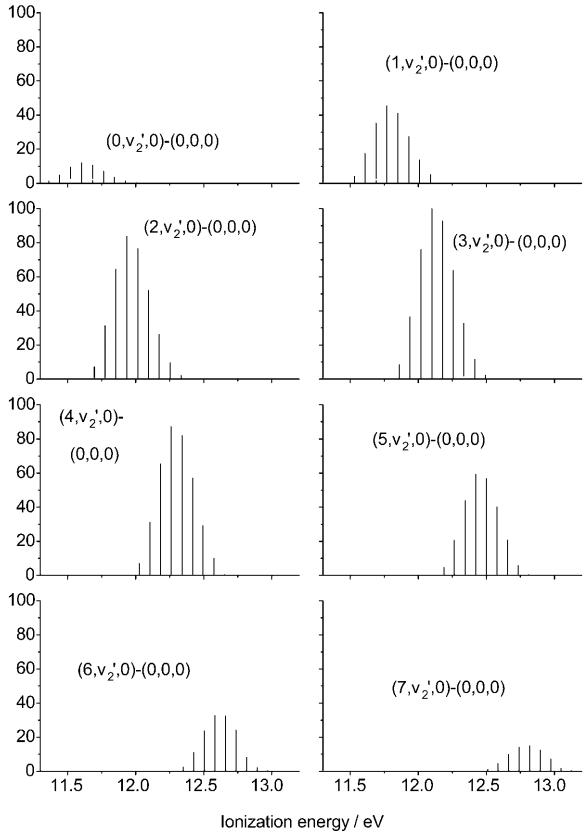

Figure 8. Computed Franck–Condon factors of eight major vibrational progressions at 0 K of the CF_2^+ ($\tilde{X}^2A_1$)+e^-←CF_2 ($\tilde{X}^1A_1$) photoionization process and their vibrational assignments.

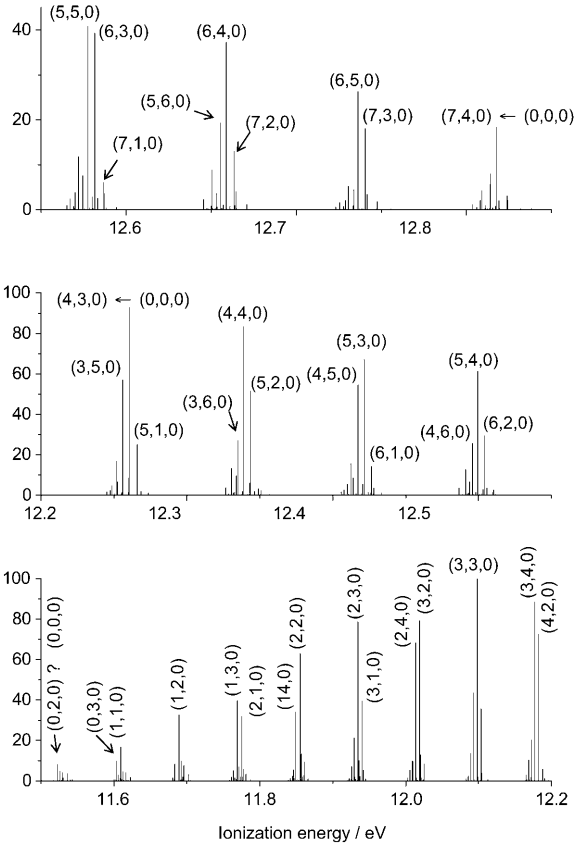

Figure 9. Computed Franck–Condon factors of the CF_2^+ ($\tilde{X}^2A_1$)+e^-←CF_2 ($\tilde{X}^1A_1$) photoionization process in the 11.5–12.9 eV IE region, and vibrational assignments of some vibrational components, which contribute to some of the doublet structures in the observed threshold photoelectron spectrum (see text).

there are a number of "hot" band components, namely the (0,1,0)←(0,1,0), (1,0,0)←(0,2,0) and (0,2,0)←(1,0,0) components at computed ionization energies of 11.359, 11.363 and 11.370 eV, respectively, which are very close to the (0,0,0)← (0,0,0) component at 11.362 eV. However, in order to resolve the vibrational structure in this congested region, a better experimental resolution than 5 meV FWHM is required.

An overview of the assignment of the main structure in the experimental TPE spectrum in the photon energy region 11.3–12.2 eV is shown in Figure 11. As can be seen, the main structure shown corresponds to (v_1',v_2',0)←(0,0,0) combination bands with $v' = 0$, 1, 2 and 3. The doublet structure observed in some of these bands arises because $2\nu_2'$ is approximately equal to ν_1'. On comparing Figure 11 with the experimental TPE spectrum in the photon energy region 11.4–12.2 eV (Figure 6), and using the information provided in the simulations in Figures 9 and 10, the doublet structure observed in the experimental vibrational components can be assigned. For example, in the first two observed components at 11.45 and 11.52 eV the doublet structure can be assigned to the (0,1,0)←(0,0,0) and (1,0,0)←(0,1,0) ionizations, and the (0,2,0)←(0,0,0) and (1,2,0)←(1,0,0), respectively. Also, the doublet structure in the band at 11.77 eV can be assigned to the ionizations (1,3,0)←(0,0,0) and (2,1,0)← 0,0,0).

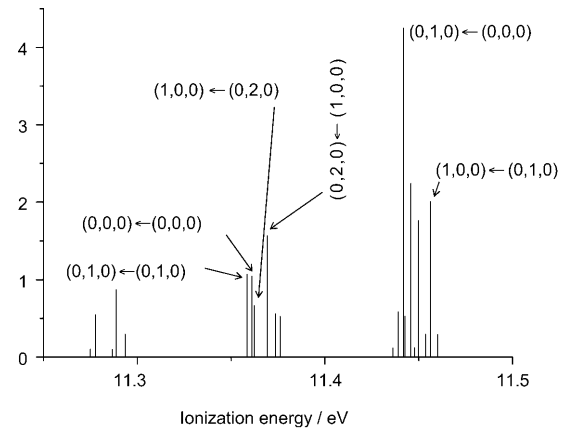

Figure 10. Computed Franck–Condon factors of the CF_2^+ ($\tilde{X}^2A_1$)+e^-←CF_2 ($\tilde{X}^1A_1$) photoionization process and assignments of some vibrational components in the AIE region.

Once the main assignments of the structure in the experimental TPE spectrum have been established, values of the vibrational constants ν_1' (sym. stretching mode) and ν_2' (sym. bending mode) in the ionic state can be derived. For ν_1', ω_e and $\omega_e x_e$ were obtained as (1370±20) and (7±10)

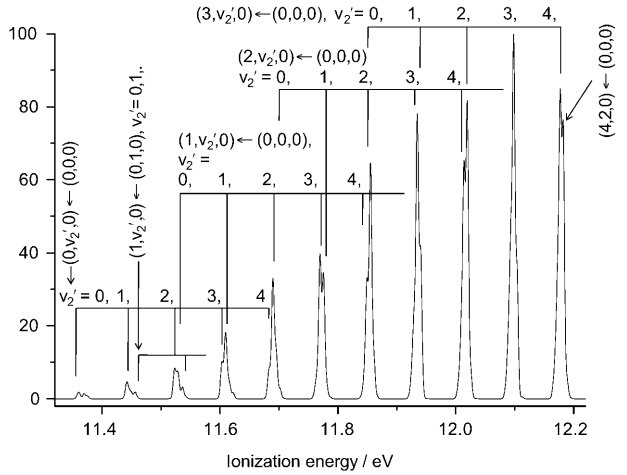

Figure 11. A simulated spectrum showing assignment of the main structure in the low energy region (11.3–12.2 eV) in the first photoelectron band of CF_2. The doublet structure observed in some of the bands arises because $2\nu_2'$ is approximately equal to ν_1'. More detail of the structure in the band at 11.36 eV is shown in Figure 10. The main structure shown corresponds to $(v_1',v_2',0)\leftarrow(0,0,0)$ combination bands with $v'=0$, 1, 2 and 3.

cm^{-1}. The value for ω_e, compares very well with the value of 1370.0 cm^{-1} obtained from the CAS/MRCI/aug-cc-pV5Z PEF while the fundamental separation (1356±20) cm^{-1} also compares very well with the value of 1356.3 cm^{-1} derived from the CAS/MRCI/aug-cc-pV5Z PEF (see values listed in Table 1). The agreement is not so good for ν_2'. The harmonic and fundamental values expected from the CAS/MRCI/aug-cc-pV5Z PEF are 653.2 and 651.7 cm^{-1} respectively. The corresponding ω_e and $\omega_e x_e$ values obtained from the experimental TPE spectrum are (635±10) cm^{-1} and (0±5) cm^{-1}, giving the harmonic and fundamental values as (635±10) cm^{-1}.

This work indicates that studies with TPE spectroscopy, supported by ab initio/Franck–Condon calculations, of other tri- and tetra-atomic reactive intermediates, in which vibrational structure in more than one vibrational mode in the first and higher PE bands is expected, is possible and this is planned for future work. Possible reactive intermediates that could be studied in this way include HO_2,[43] HNO,[44] HCO,[45] CH_2Cl and $CHCl_2$.[46] In each case, the results should lead to a more reliable determination of the AIE, assignment of the observed vibrational structure and hence determination of vibrational frequencies in the ionic state.

Conclusion

In this work, the first photoelectron band of difluorocarbene, CF_2, has been recorded with threshold photoelectron (TPE) spectroscopy. Extensive vibrational structure was obtained for this band but the adiabatic component was not observed. Even though the TPE vibrational envelope is non-Franck–Condon in nature, comparison of the structure seen in the vibrational components with that expected from an ab initio/Franck–Condon simulation has allowed the upper state vibrational quantum numbers associated with each observed vibrational component to be determined. The position of the adiabatic component could then be determined. Also, the harmonic and fundamental vibrational frequencies for ν_1' and ν_2' for the ionic state, CF_2^+ ($\tilde{X}^2A_1$), have been derived from the experimental TPE spectrum. These compare well with those determined from the potential energy function for CF_2^+ ($\tilde{X}^2A_1$) computed in this work with high level electronic structure calculations.

The adiabatic ionization energy of CF_2 is recommended as 11.362±0.005 eV.

Acknowledgements

The authors are grateful to EPSRC for supporting this work (grant no. EP/C515706/1), and for the provision of computational resources from the National Service for Computational Chemistry. This work was also supported by a grant from the Research Grants Council (RGC) of the Hong Kong Special Administrative Region (competitive earmarked research grant (CERG) 2007–2008 grant no. 500207). We also thank Dr. N. Zema and the technical staff of the Polar beamline (4.2R) at Elettra, Trieste for help and advice. M.E. thanks the EU Early Stage Research Training Network (SEARCHERS) for financial support.

[1] D. S. King, P. K. Schenck, J. C. Stephenson, *J. Mol. Spectrosc.* **1979**, *78*, 1.
[2] C. W. Mathews, *J. Chem. Phys.* **1966**, *45*, 1068.
[3] C. W. Mathews, *J. Chem. Phys.* **1967**, *46*, 2355.
[4] P. Venkateswarlu, *Phys. Rev.* **1950**, *77*, 676.
[5] A. Charo, F. C. De Lucia, *J. Mol. Spectrosc.* **1982**, *94*, 363.
[6] W. H. Kirchoff, D. R. Lide, Jr., F. X. Powell, *J. Mol. Spectrosc.* **1973**, *47*, 491.
[7] H. B. Qian, P. B. Davies, *J. Mol. Spectrosc.* **1995**, *169*, 201.
[8] J. B. Burkholder, C. J. Howard, P. A. Hamilton, *J. Mol. Spectrosc.* **1988**, *127*, 362.
[9] P. B. Davies, P. A. Hamilton, J. M. Elliott, M. J. Rice, *J. Mol. Spectrosc.* **1983**, *102*, 193.
[10] P. B. Davies, W. Lewis-Bevan, D. K. Russell, *J. Chem. Phys.* **1981**, *75*, 5602.
[11] J. P. Booth, G. Cunge, P. Chabert, N. Sadeghi, *J. Appl. Phys.* **1999**, *85*, 3097.
[12] B. A. Cruden, K. K. Gleason, H. H. Sawin, *J. Appl. Phys.* **2001**, *89*, 915.
[13] J. P. Booth, G. Cunge, F. Neuilly, N. Sadeghi, *Plasma Sources Sci. Technol.* **1998**, *7*, 423.
[14] M. Haverlag, E. Stoffels, W. W. Stoffels, G. M. W. Kroesen, F. J. de Hoog, *J. Vac. Sci. Technol. A* **1996**, *14*, 384.
[15] J. Röpcke, G. Lombardi, A. Rousseau, P. B. Davies, *Plasma Sources Sci. Technol.* **2006**, *15*, S148.
[16] a) I. M. P. Aarts, B. Hoex, A. H. M. Smets, R. Engeln, W. M. M. Kesssels, M. C. M. van de Sanden, *Appl. Phys. Lett.* **2004**, *84*, 3079; b) D. Romanini, A. A. Kachanov, N. Sadeghi, F. Stoeckel, *Chem. Phys. Lett.* **1997**, *264*, 316.
[17] J. P. Booth, *Plasma Sources Sci. Technol.* **1999**, *8*, 249.
[18] J. M. Dyke, L. Golob, N. Jonathan, A. Morris, M. Okuda, *J. C. S. Faraday* **1974**, *70*, 1828.
[19] T. J. Buckley, R. D. Johnson, R. E. Huie, Z. Zhang, S. C. Kuo, R. B. Klemm, *J. Phys. Chem.* **1995**, *99*, 4879.
[20] V. Tarnovsky, K. Becker, *J. Chem. Phys.* **1993**, *98*, 7868.
[21] F. Innocenti, M. Eypper, S. Beccacei, A. Morris, S. Stranges, J. B. West, G. C. King, J. M. Dyke, *J. Phys. Chem.* **2008**, *112*, 6939.
[22] F. Innocenti, L. Zuin, M. L. Costa, A. A. Dias, A. Morris, S. Stranges, J. M. Dyke, *J. Chem. Phys.* **2007**, *126*, 154310.

[23] J. M. Dyke, S. D. Gamblin, A. Morris, T. G. Wright, A. E. Wright, J. B. West, *J. Electron Spectrosc. Relat. Phenom.* **1998**, *97*, 5.
[24] J. M. Dyke, S. D. Gamblin, A. Morris, T. G. Wright, A. E. Wright, J. B. West, *J. Phys. B* **1999**, *32*, 2763.
[25] F. Innocenti, L. Zuin, M. L. Costa, A. A. Dias, M. Goubet, A. Morris, R. I. Oleriu, S. Stranges, J. M. Dyke, *Mol. Phys.* **2007**, *105*, 771.
[26] F. T. Chau, D. K. W. Mok, E. P. F. Lee, J. M. Dyke, *ChemPhysChem* **2005**, *6*, 2037.
[27] A. Halkier, T. Helgaker, W. Klopper, P. Jorgensen, A. G. Csaszar, *Chem. Phys. Lett.* **1999**, *310*, 385.
[28] J. Wormhoudt, K. E. McCurdy, J. B. Burkholder, *Chem. Phys. Lett.* **1989**, *158*, 480; C. W. Mathews, *Can. J. Phys.* **1967**, *45*, 2355; O. Suto, J. Steinfeld, *Chem. Phys. Lett.* **1990**, *168*, 181 (Data from NIST Standard Reference Database 69, June 2005 Release: NIST Chemistry WebBook; http://webbook.nist.gov/chemistry/).
[29] J. K. G. Watson, *Mol. Phys.* **1968**, *15*, 479.
[30] D. K. W. Mok, E. P. F. Lee, F. T. Chau, J. M. Dyke, *J. Chem. Phys.* **2004**, *120*, 1292.
[31] L. Margules, J. Demaison, J. E. Boggs, *J. Phys. Chem. A* **1999**, *103*, 7632.
[32] MOLPRO is a package of ab initio programs written by H.-J. Werner, P. J. Knowles, R. Lindh, F. R. Manby, M. Schütz, P. Celani, T. Korona, G. Rauhut, R. D. Amos, A. Bernhardsson, A. Berning, D. L. Cooper, M. J. O. Deegan, A. J. Dobbyn, F. Eckert, C. Hampel, G. Hetzer, A. W. Lloyd, S. J. McNicholas, W. Meyer, M. E. Mura, A. Nicklaß, P. Palmieri, R. Pitzer, U. Schumann, H. Stoll, A. J. Stone, R. Tarroni, T. Thorsteinsson, **2008**.
[33] G. K. Jarvis, K. J. Boyle, C. A. Mayhew, R. P. Tuckett, *J. Phys. Chem. A* **1998**, *102*, 3230.
[34] L. Golob, PhD thesis, University of Southampton (UK), **1975**.
[35] S. Eden, P. Limao-Vieira, P. A. Kendall, N. J. Mason, J. Delwiche, M. J. Hubin-Franskin, T. Tanaka, M. Kitajima, H. Tanaka, H. Cho, S. V. Hoffman, *Chem. Phys.* **2004**, *297*, 257.
[36] R. F. Lake, H. Thompson, *Proc. R. Soc. Lond. Ser. A* **1970**, *315*, 323.
[37] G. C. King, M. Zubek, P. M. Rutter, F. H. Read, *J. Phys. E* **1987**, *20*, 440.
[38] R. I. Hall, A. McConkey, K. Ellis, G. Dawber, L. Avaldi, M. A. MacDonald, G. C. King, *Meas. Sci. Technol.* **1992**, *3*, 316.
[39] P. M. Guyon, R. Spohr, W. A. Chupka, J. Berkowitz, *J. Chem. Phys.* **1976**, *65*, 1650.
[40] T. Baer, P. M. Guyon, *J. Chem. Phys.* **1986**, *85*, 4765.
[41] Z. L. Cai, *Theor. Chim. Acta* **1993**, *86*, 249.
[42] K. Sendt, G. B. Bacskay, *J. Chem. Phys.* **2000**, *112*, 2227.
[43] J. M. Dyke, A. Morris, N. Jonathan, M. J. Winter, *Mol. Phys.* **1981**, *44*, 1059.
[44] J. Baker, V. Butcher, J. M. Dyke, A. Morris, *J. C. S. Faraday Trans.* **1990**, *86*, 3843.
[45] J. M. Dyke, A. Morris, N. Jonathan, M. J. Winter, *Mol. Phys.* **1981**, *44*, 1059.
[46] L. Andrews, J. M. Dyke, N. Jonathan, N. Keddar, A. Morris, *J. Am. Chem. Soc.* **1984**, *106*, 299.

Received: August 15, 2008
Published online: November 12, 2008

